$[Ni_{23}Se_{12}(PEt_3)_{13}]$ Re-visited: Isolation and Characterization of $[Ni_{23}Se_{12}Cl_3(PEt_3)_{10}]$

*Alexander J. Touchton, Guang Wu, Trevor W. Hayton**

Department of Chemistry and Biochemistry, University of California, Santa Barbara, California 93106, United States

Abstract

Reaction of [Ni(1,5-COD)$_2$] (1.0 equiv), PEt$_3$ (0.04 equiv), SePEt$_3$ (0.52 equiv), and [NiCl$_2$(PEt$_3$)$_2$] (0.07 equiv) in a mixture of toluene and THF results in the formation of [Ni$_{23}$Se$_{12}$Cl$_3$(PEt$_3$)$_{10}$] (**1**), which can be isolated in moderate yield after work-up. Complex **1** was characterized by NMR spectroscopy, ESI-MS, and X-ray crystallography. This open-shell nanocluster features a central [Ni$_{13}$]$^{7+}$ anti-cuboctahedral kernel, which is encapsulated by a [Ni$_{10}$(μ-Se)$_9$Cl$_3$]$^-$ shell, along with ten PEt$_3$ ligands and three (μ$_4$-Se)$^{2-}$ ligands. On the basis of our spectroscopic and crystallographic analysis, coupled with *in situ* spectroscopic monitoring, we believe that the previously reported nanocluster, [Ni$_{23}$Se$_{12}$(PEt$_3$)$_{13}$], is actually better formulated as [Ni$_{23}$Se$_{12}$Cl$_3$(PEt$_3$)$_{10}$].

Introduction

Atomically-precise nanoclusters (APNCs) of the group 11 metals have garnered considerable attention in the last decade.[1-8] A common structural feature of these materials is the presence of [M_{13}] cuboctahedral, anti-cuboctahedral, or icosahedral kernels. For example, the archetypal Au APNC, [$NOct_4$][$Au_{25}(SCH_2CH_2Ph)_{18}$] features a icosahedral [Au_{13}] core.[9-10] However, this structural feature is uncommon outside of the coinage metal triad, and is even rarer for the 1st row transition metals, Fe, Co, and Ni. For example, to our knowledge, only two nickel clusters possess comparable [M_{13}] kernels, namely, [$Ni_{23}Se_{12}(PEt_3)_{13}$], reported in 1992 by Steigerwald and co-workers,[11] and [$Ni_{21}Se_{14}(PEt_2Ph)_{12}$], reported in 1992 by Fenske and co-workers.[12] These clusters feature anti-cuboctahedral and cuboctahedral [M_{13}] kernels, respectively. Other notable examples of Ni APNCs with a high degree of metal-metal bonding include [$HNi_{38}(CO)_6(\mu\text{-}CO)_{36}C_6]^{5-}$, [$Ni_{32}C_6(CO)_{36}]^{6-}$, and [$Ni_9Te_6(PEt_3)_8$].[13-16] The latter example features a cubic [M_9] kernel in which the central Ni atom is only bound by Ni metal atoms.[16] The closely related Co cluster, [$Co_9Te_6(CO)_8$], is also known.[17]

Scheme 1. Reported Synthesis of [$Ni_{23}Se_{12}(PEt_3)_{13}$]

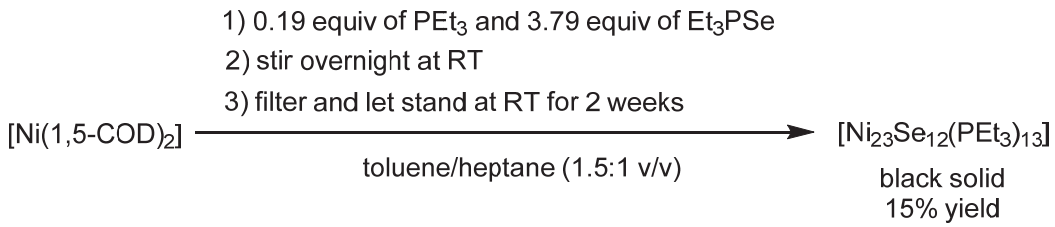

Given our current interest in the synthesis of APNCs of Co and Ni,[18-22] we set out to remake [$Ni_{23}Se_{12}(PEt_3)_{13}$].[11] This cluster was originally synthesized by reaction of [$Ni(1,5\text{-}COD)_2$] with 0.19 equiv of PEt_3 and 3.79 equiv of Et_3PSe in toluene/heptane (Scheme 1). Crystals of

[$Ni_{23}Se_{12}(PEt_3)_{13}$] were grown by allowing the reaction mixture to stand undisturbed for 2 weeks and could be isolated in 15% yield. The cluster was characterized by single-crystal X-ray diffraction, elemental analysis, and SQUID magnetometry,[23] but NMR spectroscopic and mass spectrometric data, the latter being especially useful in APNC characterization, were not included in the original report. In addition, the original X-ray data for [$Ni_{23}Se_{12}(PEt_3)_{13}$] was of insufficient quality to locate all of the carbon atoms of the PEt_3 ligands.

Herein, we describe the synthesis and characterization of [$Ni_{23}Se_{12}Cl_3(PEt_3)_{10}$] (**1**), formed during an attempt to remake [$Ni_{23}Se_{12}(PEt_3)_{13}$]. Our characterization of **1** by NMR spectroscopy, electrospray ionization mass spectrometry (ESI-MS), solution-state magnetometry, elemental analysis, and X-ray crystallography, coupled with our attempts to repeat the synthesis of [$Ni_{23}Se_{12}(PEt_3)_{13}$], suggest to us that the latter complex was originally misidentified and is better formulated as [$Ni_{23}Se_{12}Cl_3(PEt_3)_{10}$] (**1**).

Results and Discussion

We first attempted to prepare [$Ni_{23}Se_{12}(PEt_3)_{13}$] using a slightly modified experimental procedure. Thus, a toluene solution of [Ni(1,5-COD)$_2$] (1.0 equiv) and PEt_3 (0.38 equiv) was treated with elemental Se (0.53 equiv) in toluene (Scheme 2a). For comparison, the original experimental procedure used $SePEt_3$ as both the Se and PEt_3 sources.[11] Filtration of the reaction mixture after 4 d, followed by crystallization from THF at –25 °C, resulted in isolation of a few dark brown crystals. These crystals were identified as [$Ni_{23}Se_{12}Cl_3(PEt_3)_{10}$] (**1**) on the basis of an X-ray crystallographic analysis (see below). Importantly, the unit cell parameters for these crystals are indistinguishable from those provided for [$Ni_{23}Se_{12}(PEt_3)_{13}$] by Steigerwald and co-workers.[11] The formulation of **1** was further confirmed by ESI-mass spectrometry. In particular,

the ESI-MS spectrum (positive ion mode, capillary voltage of 2.50 kV) of these crystals, dissolved in THF, displays prominent peaks at 3585.45 *m/z*, which is assignable to $[\mathbf{1}]^+$, and 3629.39 *m/z*, which is assignable to $[\mathbf{1} - Cl + Br]^+$ (Figures S36–S39).[24] Unfortunately, only trace amounts of **1** could be isolated using this synthetic procedure, which is not surprising, given that only adventitious quantities of Cl^- are present in the reaction mixture. Several other authors have noted the incorporation of adventitious Cl^- into their molecules, from a variety of sources.[18, 25-29] In our case, we suggest that CH_2Cl_2 in our glovebox atmosphere is the source of the Cl^- ions. This hypothesis is consistent with the observed reactivity of **1** (and presumably other low-valent Ni APNCs) with CH_2Cl_2 (see below), as well as the small quantities of CH_2Cl_2 that would be necessary to generate **1** (only 0.0032 equiv of CH_2Cl_2 would be necessary to generate **1** in 5% yield, assuming each CH_2Cl_2 donates both of its Cl atoms).

Scheme 2. Syntheses of $[Ni_{23}Se_{12}Cl_3(PEt_3)_{10}]$ (**1**) performed (a) without; and (b) with an exogenous Cl^- source.

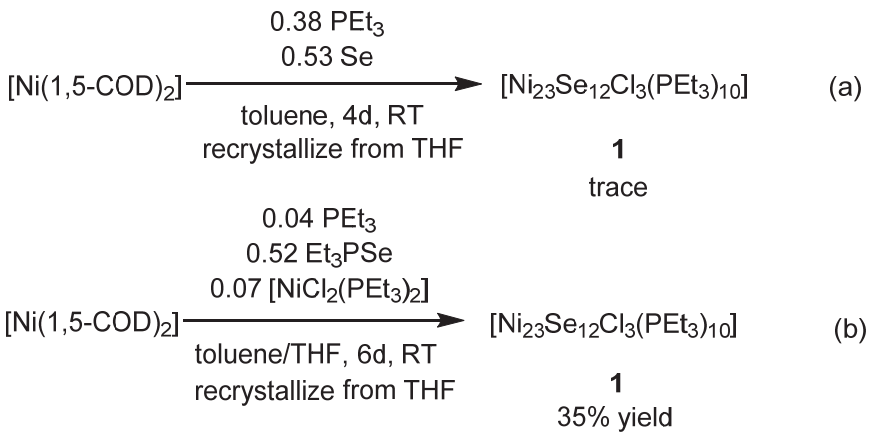

In an effort to develop a rational, higher-yielding synthesis of **1**, we performed the reaction in the presence of $[NiCl_2(PEt_3)_2]$,[30] which we hypothesized could serve as a Cl^- source. Thus, a toluene solution of $[Ni(1,5\text{-}COD)_2]$ (1.0 equiv), PEt_3 (0.04 equiv), and $SePEt_3$ (0.52 equiv) was

allowed to stir for 30 min, whereupon $[NiCl_2(PEt_3)_2]$ (0.07 equiv) and THF were added to the reaction mixture (Scheme 2b). Work-up of this solution after 6 d resulted in isolation of **1** in 35% yield as a dark brown crystalline solid. Importantly, the isolated single crystals of **1** prepared with $[NiCl_2(PEt_3)_2]$ have identical ESI-MS spectral data to the single crystals of **1** prepared without $[NiCl_2(PEt_3)_2]$ (see below for further discussion), confirming their identical formulations. Complex **1** is sparingly soluble in benzene, toluene, and THF, and insoluble in pentane, hexanes, diethyl ether, and acetonitrile. It is soluble in CH_2Cl_2; however, it quickly reacts with this solvent, forming a new paramagnetic product over the course of a few hours (Figure S50).

Complex **1** crystallizes in the trigonal *R*3*c* space group as a THF solvate, **1**·3THF. It exhibits crystallographically-imposed C_3 symmetry in the solid-state (Figure 1a and 1g). Complex **1** is isostructural with previously reported cluster, $[Ni_{23}Se_{12}(PEt_3)_{13}]$, except that three phosphorus atoms in $[Ni_{23}Se_{12}(PEt_3)_{13}]$ have been replaced by three chlorine atoms in **1**. Complex **1** features a central $[Ni_{13}]^{7+}$ anti-cuboctahedral kernel (Figures 1b-d). One hemisphere of the $[Ni_{13}]^{7+}$ kernel is encapsulated by a $[Ni_{10}(\mu\text{-}Se)_9Cl_3]^-$ shell (Figures 1e and 1f). Additionally, there are seven PEt_3 ligands attached to the $[Ni_{10}(\mu\text{-}Se)_9Cl_3]^-$ shell in two inequivalent groups: six located along the equatorial belt and one at the apex. These PEt_3 ligands are bound to Ni1, Ni2, and Ni4, along with their symmetry-related counterparts (See Figure S1 for atom labelling scheme). The other hemisphere of the $[Ni_{13}]^{7+}$ kernel is bound by three $(\mu_4\text{-}Se)^{2-}$ ligands and three PEt_3 ligands. The $(\mu_4\text{-}Se)^{2-}$ ligands occupy the square faces of the anti-cuboctahedron, whereas the PEt_3 ligands are bound to Ni3 and its two symmetry-related counterparts, giving rise to a C_3-symmetric [*cyclo*-$Ni_3(\mu\text{-}Se)_3(PEt_3)_3$] terrace. The average Ni–Ni distance in **1** is 2.57(4) Å (range = 2.348(6) - 2.814(6) Å). For comparison, the average Ni–Ni distances in $[Ni_{23}Se_{12}(PEt_3)_{13}]$ and bulk Ni

metal are 2.55 (range = 2.346(6) - 2.831(6) Å) and 2.49 Å, respectively.[11, 31] For further comparison, the average Ni–Ni distances in $[Ni_{21}Se_{14}(PEt_2Ph)_{12}]$ and $[Ni_{34}Se_{22}(PPh_3)_{10}]$ are 2.64 and 2.77 Å, respectively.[12, 32]

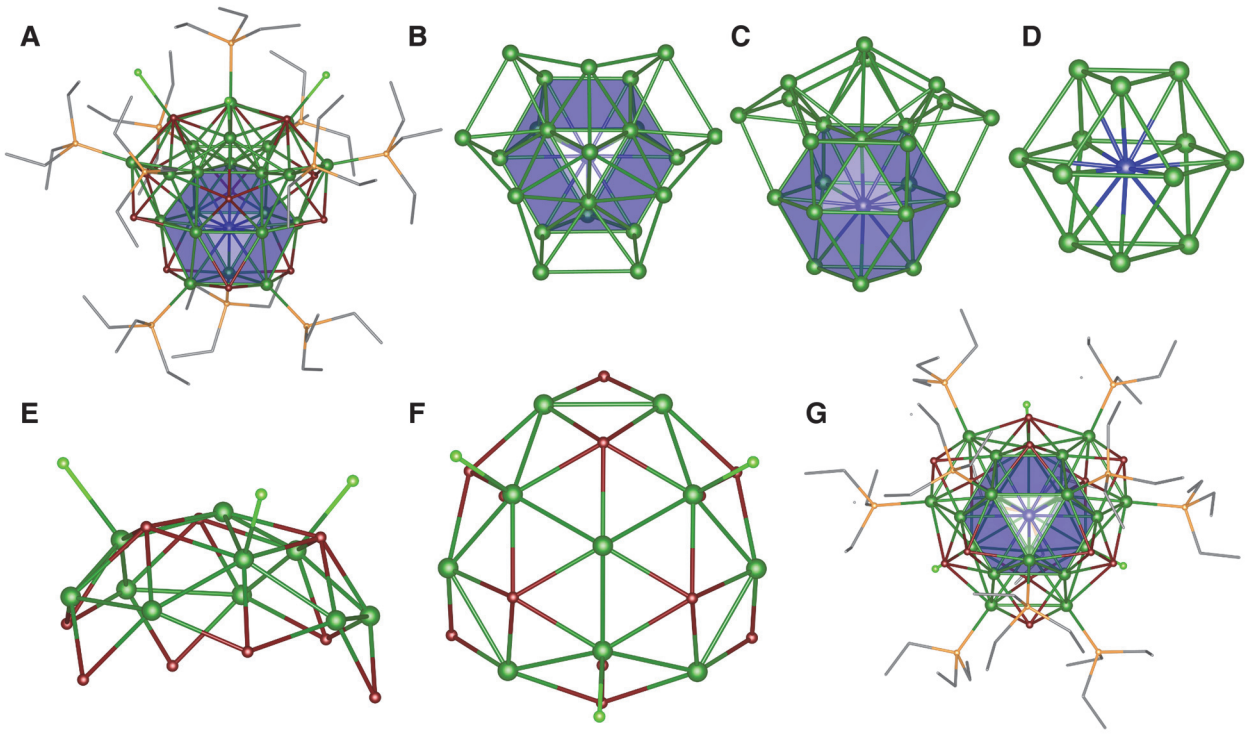

Figure 1. Ball and stick structure of $[Ni_{23}Se_{12}Cl_3(PEt_3)_{10}]$·3THF (**1**·3THF). Ni atoms are shown in green, except for the central Ni atom, which is shown in blue. The blue polyhedron represents the coordination sphere of the central Ni atom. P, Se, and Cl atoms are shown in orange, maroon, and bright green, respectively. C atoms are depicted in grey wireframe. Hydrogen atoms and THF solvate atoms are omitted for clarity. (a) and (g) show **1**·3THF perpendicular to the C_3 axis and along the C_3 axis, respectively. (b) and (c) show the $[Ni_{23}]$ core along the C_3 axis and perpendicular to the C_3 axis, respectively. (d) shows the $[Ni_{13}]^{7+}$ anti-cuboctahedral kernel. (e) and (f) show the $[Ni_{10}(\mu\text{-}Se)_9Cl_3]^-$ shell attached to the $[Ni_{13}]^{7+}$ kernel from two different views.

Complex **1** also features six Se^{2-} ligands that adopt μ_4 binding modes and six Se^{2-} ligands that adopt μ_5 binding modes. The average Ni–Se distance in **1** is 2.39(4) Å (range = 2.299(5) - 2.478(5) Å). For comparison, the average Ni–Se distances in $[Ni_{23}Se_{12}(PEt_3)_{13}]$, bulk Ni_3Se_2, and bulk NiSe are 2.39 (range = 2.303(2) - 2.477(9) Å), 2.37, and 2.50 Å, respectively.[33-34] In addition, the average Ni–P distance in **1** is 2.21(3) Å (range = 2.219(8) - 2.247(15) Å), whereas the Ni5–Cl1 distance is 2.274(8) Å (Figure S1). For comparison, the average Ni–P distance in $[Ni_{23}Se_{12}(PEt_3)_{13}]$ is 2.22(1) Å (range = 2.21(1) - 2.268(7) Å), excluding the Ni8–P4 distance. This distance, which corresponds Ni–Cl bond in complex **1**, is 2.271(3) Å. For further comparison, the average Ni–Cl distances in $[Ni_5Se_4Cl_2(PEt_2Ph)_6]$, $[Ni_8S_6Cl_2(PPh_3)_6]$, and $[Ni_3Se_2Cl_2(PEt_3)_4]$ (**2**, see below) are 2.22, 2.20, and 2.23 Å, respectively.[12, 35-36] These shorter values likely reflect the lower coordination number of the Ni atoms in these examples.

The ^{31}P NMR spectrum of **1** in THF-d_8 at 25 °C consists of two paramagnetically-shifted resonances at 477 and 1081 ppm, in a 3:6 ratio, respectively (Figures S43). These resonances are assignable to the three PEt_3 ligands bound to the [*cyclo*-$Ni_3(\mu\text{-}Se)_3(PEt_3)_3$] terrace and the six PEt_3 ligand located along the equatorial belt. The resonance assignable to the PEt_3 ligand located at the apex of the $[Ni_{10}(\mu\text{-}Se)_9Cl_3]^-$ shell was not observed, presumably due to paramagnetic broadening. The ^1H NMR spectrum of **1** in C_6D_6 at 25 °C displays a broad resonance at 43.19 ppm, which is assignable to the methylene groups of the apical PEt_3 ligand. Also present in the spectrum are broad multiplets at 5.75 and 5.50 ppm, which are assignable to the diastereotopic methylene protons of the six equatorial PEt_3 ligands. The spectrum also features a broad singlet at 3.69 ppm, which is assignable to the methylene groups of the three PEt_3 ligands located in the [*cyclo*-$Ni_3(\mu\text{-}Se)_3(PEt_3)_3$] terrace (Figure S40). These four resonances are present in a 1:3:3:3 ratio, which is consistent with our proposed formulation. Additionally, we observe resonances at

6.87 ppm, 1.82, and 1.17 ppm, in a 1:6:3 ratio, which are assignable to the methyl groups of the three expected PEt_3 environments. A solution-state magnetic moment of 3.68 μ_B was measured for **1** in THF-d_8 at 25 °C by Evans' method,[37-38] which is close to the value expected for 3 unpaired electrons (3.87 μ_B). This moment is much larger than the moment reported for $[Ni_{23}Se_{12}(PEt_3)_{13}]$ (2.3 μ_B);[23] a discrepancy that we have been unable to rationalize. Finally, the ESI-MS of crystalline **1** in THF features a peak at 3585.65 *m/z* (calcd 3585.30 *m/z*) corresponding to $[\mathbf{1}]^+$ (Figure 2), further corroborating our formulation. Crucially, a peak assignable to $[Ni_{23}Se_{12}(PEt_3)_{13}]^+$ (calcd 3832.67 *m/z*) is not observed in this spectrum (Figure S49).

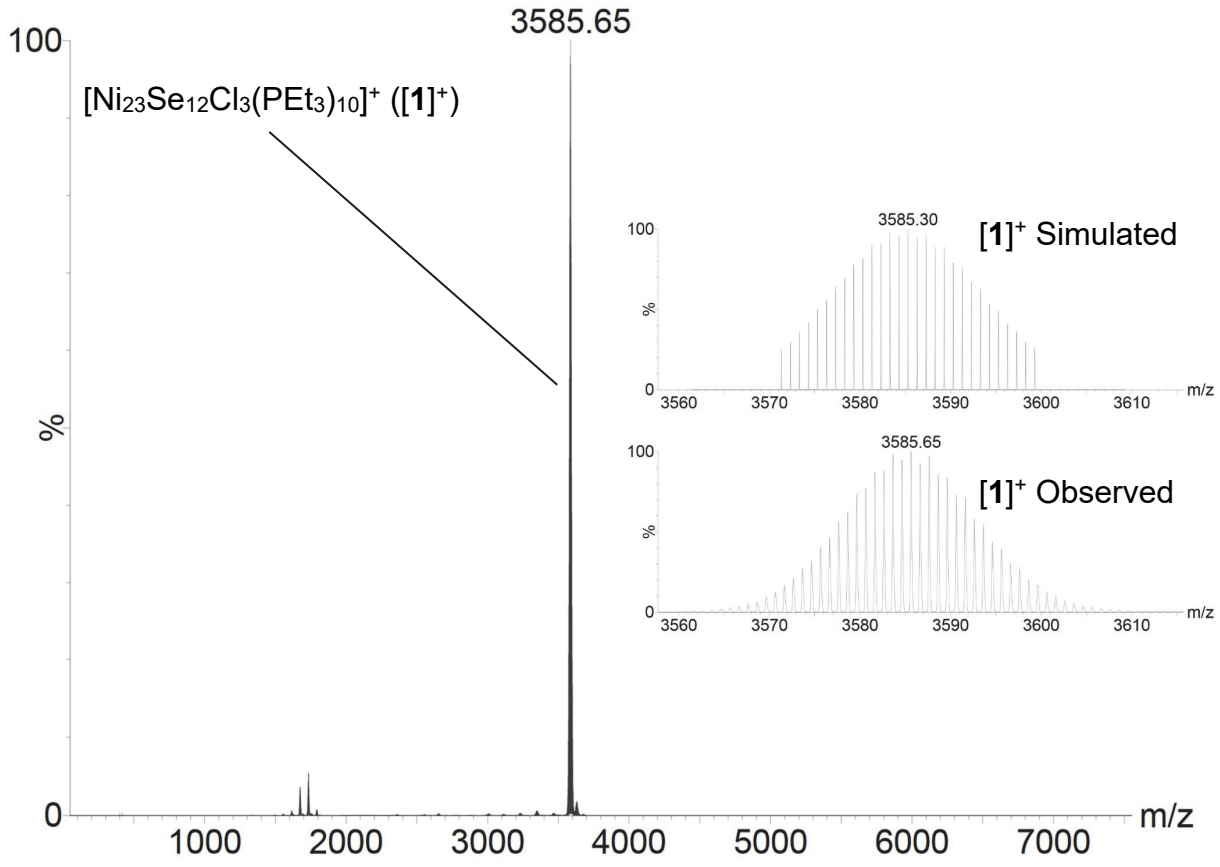

Figure 2. ESI-MS spectrum of $[Ni_{23}Se_{12}Cl_3(PEt_3)_{10}]$ (**1**), recorded in THF in positive ion mode at a capillary voltage of 2.50 kV.

In an effort to rationalize the moderate yields of **1**, we recorded a $^{31}P\{^1H\}$ NMR spectrum of the reaction mixture in C_6D_6 before work-up (Figure S56). This spectrum features resonances at 509 and 43.1 ppm, which are assignable to **1** and unreacted $SePEt_3$,[39] respectively. Also present in this spectrum are resonances at 13.6 and 12.7 ppm, which are present in a 1:1 ratio, and which are assignable to the trimetallic cluster, $[Ni_3(\mu_3\text{-}Se)_2Cl_2(PEt_3)_4]$ (**2**). Importantly, the observation of **2** in the spectrum helps explain the modest yields of **1**, because its formation sequesters Cl^-, which is only added in stoichiometric amounts to the reaction mixture. Despite several attempts, we have not found reaction conditions that completely suppress the formation of **2**. We are also unsure if complex **2** is an intermediate in the formation of **1** or a side-product of the reaction.

Scheme 3. Synthesis of $[Ni_3(\mu_3\text{-}Se)_2Cl_2(PEt_3)_4]$ (**2**)

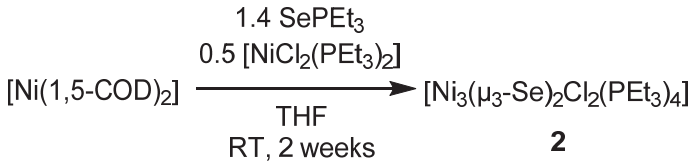

Complex **2** can be obtained red-brown plates in 3% yield from the Et_2O fraction obtained upon work-up of **1** (see SI for details). While the low yield suggests that **2** is a minor species in the reaction mixture, our NMR spectral data suggest that it is present in much larger quantities; however, it could only be isolated in crystalline form in low yield. Complex **2** can also be prepared by treatment of $[Ni(1,5\text{-}COD)_2]$ (1.0 equiv) with $SePEt_3$ (1.4 equiv) and $[NiCl_2(PEt_3)_2]$ (0.5 equiv) in THF (Scheme 3). When prepared in this fashion it can be isolated in 16% yield. It crystallizes from pentane in the monoclinic space group $P2_1/n$ (Figure 3) and is isostructural with

the previously reported group 10 sulfide clusters, $[Ni_3(\mu_3\text{-}S)_2Br_2(PEt_3)_4]$ and $[M_3(\mu_3\text{-}S)_2Cl_2(PPh_3)_4]$ (M = Ni, Pd).[40-41] Each face of the Ni_3 triangle is bridged by a $[\mu_3\text{-}Se]^{2-}$ ligand. Additionally, Ni1 and Ni3 are bound by one Cl^- ligand and one PEt_3 ligand, whereas Ni2 is bound to two PEt_3 ligands, resulting in a structure with overall C_2 symmetry. Importantly, this symmetry is consistent with the number and intensities of the $^{31}P\{^1H\}$ NMR resonances assigned to **2** (Figure S53). Each Ni atom possesses square planar geometry (Σ(∠L–Ni1–L) = 360.00°, Σ(∠L–Ni2–L) = 363.08°, Σ(∠L–Ni3–L) = 359.99°), consistent with the 2+ oxidation state expected for each metal center. Finally, the long Ni–Ni distances in **2** (Ni1–Ni2 = 3.024(1) Å, Ni2–Ni3 = 2.992(1) Å, Ni1–Ni3 = 3.238(1) Å) indicate that no Ni–Ni bonding is present.

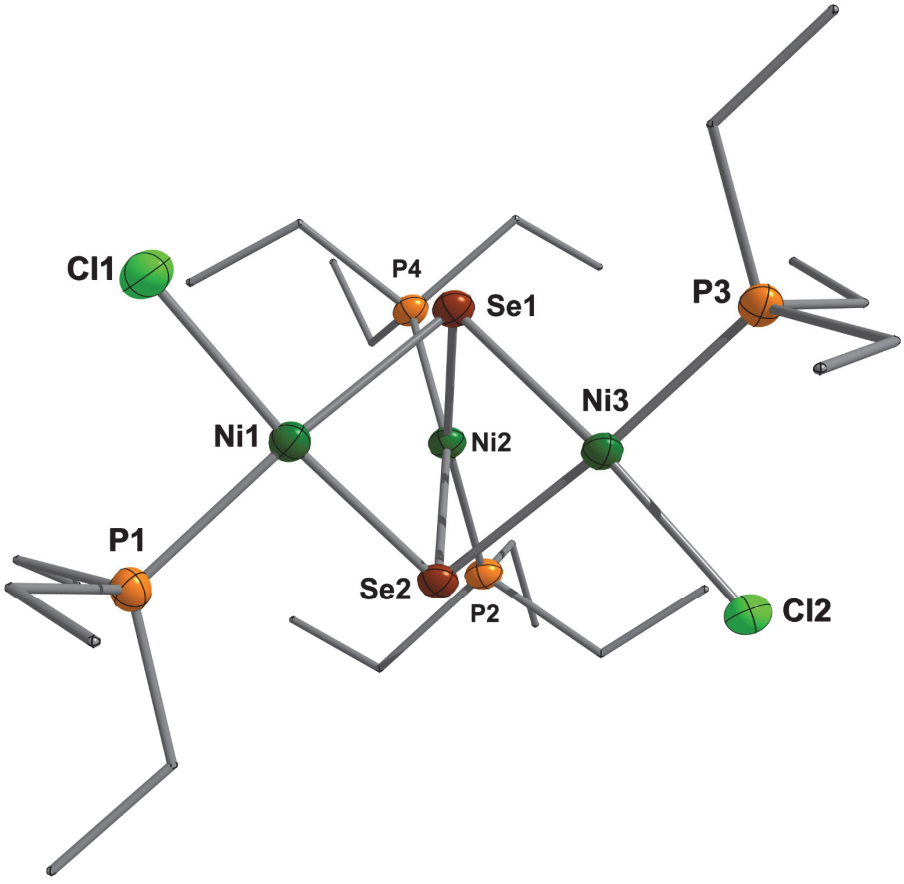

Figure 3. ORTEP diagram of $[Ni_3(\mu_3\text{-}Se)_2Cl_2(PEt_3)_4]$ (**2**) with thermal ellipsoids displayed at 50% probability for non-carbon atoms. Hydrogen atoms omitted for clarity. Carbon atoms shown in grey wireframe. Selected distances (Å) and angles (°): Ni1–Ni2 = 3.024(1), Ni2–Ni3 = 2.992(1), Ni1–Ni3 = 3.238(1), Ni1–P1 = 2.1990(13), Ni2–P2 = 2.2151(14), Ni2–P4 = 2.2116(14), Ni3–P3 = 2.1926(13), Ni3–Cl2 = 2.2214(13), Ni1–Cl1 = 2.2408(14), Ni1–Se1 = 2.3351(9), Ni1–Se2 = 2.2797(9), Ni2–Se1 = 2.3370(10), Ni2–Se2 = 2.3357(11), Ni3–Se1 = 2.2785(9), Ni3–Se2 = 2.3336(9), Σ(∠L–Ni1–L) = 360.00, Σ(∠L–Ni2–L) = 363.08, Σ(∠L–Ni3–L) = 359.99.

Given our inability to isolate a cluster matching the original $[Ni_{23}Se_{12}(PEt_3)_{13}]$ formulation, we monitored the *in situ* reaction mixture using ESI-MS, following the original synthesis conditions as closely as possible (Scheme 1). Thus, a toluene/heptane (1.5/1 v/v) solution of $[Ni(1,5\text{-}COD)_2]$ (1.0 equiv), PEt_3 (0.19 equiv), and $SePEt_3$ (3.9 equiv) was allowed to stir at room temperature for 18 h. An aliquot of the reaction mixture was collected, dried *in vacuo*, and dissolved in THF. The ESI-MS spectrum of this aliquot reveals major peaks at 1337.59, 1513.62, 1691.65, 2240.84, 2537.04, and 3420.50 *m/z* assignable to $[Ni_6Se_5(PEt_3)_5]^+$ (calcd 1337.65 *m/z*), $[Ni_7Se_5(PEt_3)_6]^+$ (calcd 1513.67 *m/z*), $[Ni_8Se_5(PEt_3)_7]^+$ (calcd 1691.70 *m/z*), $[Ni_{14}Se_9(PEt_3)_6]^+$ (calcd 2240.88 *m/z*), $[Ni_{15}Se_9(PEt_3)_8]^+$ (calcd 2537.00 *m/z*), and $[Ni_{22}Se_{12}(PEt_3)_{10}]^+$ (calcd 3420.46 *m/z*), respectively (Figures S4-S7). These formulations are supported by excellent agreement between experimental and simulated mass spectra (Figures S13–S15, S17-S18, S22). Additionally, the closely-related clusters, $[Ni_7Se_5(P^iPr_3)_6]$ and $[Ni_8S_5(PEt_3)_7]$, have been previously isolated and characterized by X-ray crystallography,[12,21] providing further support for our formulations. Also present in this spectrum are minor peaks at 3550.46 *m/z* and 3585.43 *m/z* (Figure S8), which are assignable to $[Ni_{23}Se_{12}Cl_2(PEt_3)_{10}]^+$ ([**1** - Cl]$^+$, calcd 3550.34 *m/z*) and $[Ni_{23}Se_{12}Cl_3(PEt_3)_{10}]^+$ ([**1**]$^+$, calcd 3585.30 *m/z*), respectively (Figures S23-S24). Importantly, no peaks corresponding to

$[Ni_{23}Se_{12}(PEt_3)_{13}]^+$ or $[Ni_{23}Se_{12}(PEt_3)_{13}]^{2+}$ are observed in this spectrum (Figures S9-S10), suggesting that $[Ni_{23}Se_{12}(PEt_3)_{13}]$ is not present in the sample.

The reaction mixture was filtered and allowed to stand at room temperature for 2 weeks undisturbed. An aliquot of the resulting solution was then collected, dried *in vacuo*, and dissolved in THF. The ESI-MS spectrum of this aliquot reveals substantial changes to the cluster distribution. In particular, the ESI-MS features major peaks at 2652.30 and 3008.58 *m/z*, which are assignable to $[Ni_{17}Se_9(PEt_3)_8]^+$ (calcd 2652.86 *m/z*) and $[Ni_{19}Se_{12}(PEt_3)_8]^+$ (calcd 3008.48 *m/z*), respectively (Figures S26-S27), while the peaks assignable to $[Ni_7Se_5(PEt_3)_6]^+$, $[Ni_8Se_5(PEt_3)_7]^+$, and $[Ni_{22}Se_{12}(PEt_3)_{10}]^+$ are absent from the spectra. The peaks assignable to $[Ni_{23}Se_{12}Cl_2(PEt_3)_{10}]^+$ and $[Ni_{23}Se_{12}Cl_3(PEt_3)_{10}]^+$ ($[\mathbf{1}]^+$) are also present in this spectrum, but they still remain minor species (Figures S27-28, S32-33). Importantly, there is still no peak corresponding to $[Ni_{23}Se_{12}(PEt_3)_{13}]^+$ in the spectrum, suggesting that $[Ni_{23}Se_{12}(PEt_3)_{13}]^+$ is not formed upon long reaction times. Intriguingly, the ESI-MS data suggests that even larger nanoclusters, such as $[Ni_{26}Se_{14}(PEt_3)_{10}]$, are also present in the reaction mixture (Figure S34), although they appear to be minor products.

To account for these observations, we suggest that the material isolated by Steigerwald and co-workers in 1992, and formulated as $[Ni_{23}Se_{12}(PEt_3)_{13}]$, was actually complex **1**. This hypothesis explains our isolation of **1** using nearly identical reaction conditions, along with our inability to observe a cluster with the $[Ni_{23}Se_{12}(PEt_3)_{13}]$ formulation in the *in situ* monitoring experiments. It is also consistent with the identical metrical parameters and unit cell data observed for the two clusters. This misidentification is perhaps not surprising, given the similarity of the Ni–Cl and Ni–P bond lengths in **1**/$[Ni_{23}Se_{12}(PEt_3)_{13}]$, the similar X-ray scattering power of Cl and P,[42-43] and the inability to confidently locate the carbon atoms in the original structure. Inspection of the space

filling diagram of **1** raises further doubts about the $[Ni_{23}Se_{12}(PEt_3)_{13}]$ formulation (Figure 4). In particular, the chloride ligand in **1** occupies a narrow pocket on the cluster surface formed by the ethyl groups from the neighboring PEt_3 ligands. The close approach of these ethyl groups to Cl1 (e.g., Cl1-C5 = 3.54(2) Å, Cl1-C9 = 3.62(3) Å and 3.69(4) Å) makes it unlikely that a PEt_3 ligand could occupy this binding site instead. That said, our hypothesis does not account for the reported elemental analysis of $[Ni_{23}Se_{12}(PEt_3)_{13}]$,[11] which included a phosphorus analysis, nor does it definitively explain our differing magnetic moments. Thus, it remains possible that $[Ni_{23}Se_{12}(PEt_3)_{13}]$ was indeed isolated and structurally characterized in 1992 (perhaps as an impure sample), but that we have been unable to repeat its synthesis.

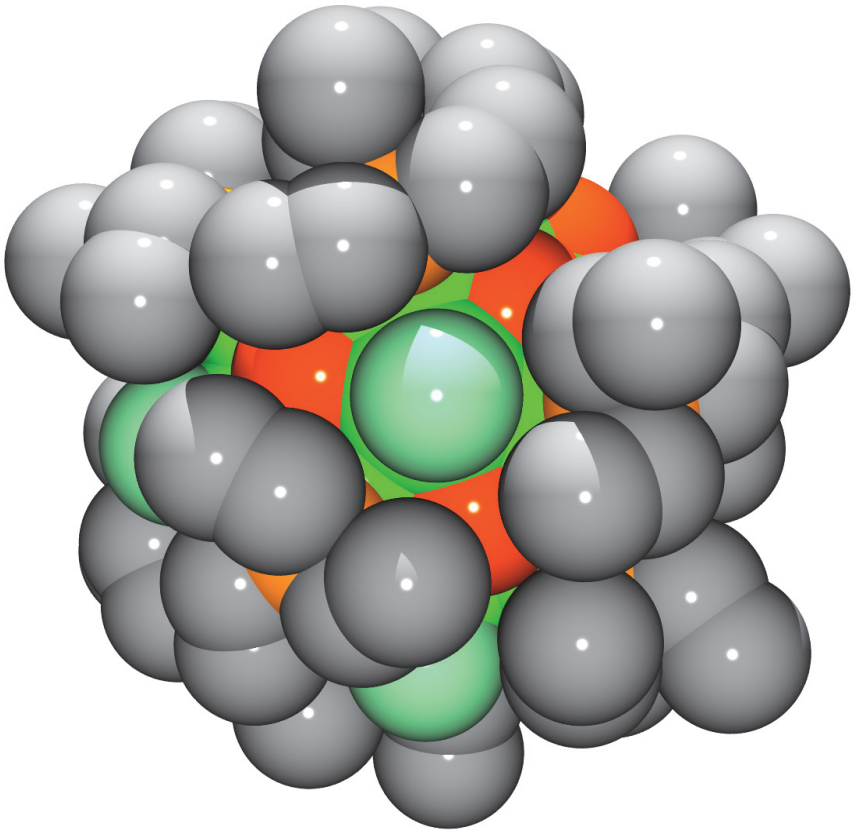

Figure 4. Space-filling diagram of $[Ni_{23}Se_{12}Cl_3(PEt_3)_{10}]\cdot 3THF$ (**1**·3THF), viewed down an Ni-Cl axis. Ni, P, Se, C, and Cl atoms are shown in green, orange, red-orange, grey, and aquamarine, respectively. Hydrogen atoms and THF solvate atoms are omitted for clarity.

Conclusion

We have synthesized and characterized the Ni_{23} nanocluster, $[Ni_{23}Se_{12}Cl_3(PEt_3)_{10}]$. Its formulation was confirmed by a combined NMR spectroscopic, mass spectrometric, and X-ray crystallographic analysis. It represents an exceptionally rare example of an APNC with a $[Ni_{13}]$ anti-cuboctahedral core. On the basis of our analysis, coupled with *in situ* spectroscopic monitoring, we believe that the cluster previously formulated as $[Ni_{23}Se_{12}(PEt_3)_{13}]$ is actually $[Ni_{23}Se_{12}Cl_3(PEt_3)_{10}]$. Our reformulation of $[Ni_{23}Se_{12}(PEt_3)_{13}]$ changes its average Ni oxidation state from +1.04 to +1.17, potentially changing the interpretation of the previously collected magnetism data. More importantly, the reproducible, rational synthesis of $[Ni_{23}Se_{12}Cl_3(PEt_3)_{10}]$ should enable the synthesis of new Ni APNCs, which have proven to be quite elusive. In this regard, our ESI-MS results demonstrate that larger APNCs, such as $[Ni_{26}Se_{14}(PEt_3)_{10}]$, are also being generated during the formation $[Ni_{23}Se_{12}Cl_3(PEt_3)_{10}]$. Going forward, we will attempt to selectively generate and isolate these intriguing products.

ASSOCIATED CONTENT

The Supporting Information is available free of charge at https://pubs.acs.org/doi/10.1021/xxxx.

- Experimental, spectroscopic, and crystallographic details for complexes **1** and **2** (PDF)

AUTHOR INFORMATION

Corresponding Author

*hayton@chem.ucsb.edu

Notes

The authors declare no competing financial interest.

ACKNOWLEDGMENT

We thank the National Science Foundation (CHE 1764345) for financial support of this work. This research made use of a 500 MHz NMR Spectrometer supported by an NSF Major Research Instrumentation (MRI) Award 1920299. The MRL Shared Experimental Facilities are supported by the MRSEC Program of the National Science Foundation under award NSF DMR 1720256; a member of the NSF-funded Materials Research Facilities Network. A. J. T. thanks the UCSB Eddleman Center for Quantum Innovation for a Graduate Student Support Grant.

REFERENCES

(1) Nguyen, T. A. D.; Jones, Z. R.; Goldsmith, B. R.; Buratto, W. R.; Wu, G.; Scott, S. L.; Hayton, T. W., A Cu_{25} Nanocluster with Partial Cu(0) Character. *J. Am. Chem. Soc.* **2015,** *137*, 13319.
(2) Du, X.; Jin, R., Atomically Precise Metal Nanoclusters for Catalysis. *ACS Nano* **2019,** *13*, 7383.
(3) Yao, Q.; Chen, T.; Yuan, X.; Xie, J., Toward Total Synthesis of Thiolate-Protected Metal Nanoclusters. *Acc. Chem. Res.* **2018,** *51*, 1338.
(4) Kang, X.; Zhu, M., Structural Isomerism in Atomically Precise Nanoclusters. *Chem. Mater.* **2021,** *33*, 39.
(5) Yang, J.; Jin, R., New Advances in Atomically Precise Silver Nanoclusters. *ACS Mater. Lett.* **2019,** *1*, 482.
(6) Kang, X.; Li, Y.; Zhu, M.; Jin, R., Atomically precise alloy nanoclusters: syntheses, structures, and properties. *Chem. Soc. Rev.* **2020,** *49*, 6443.

(7) Liu, X.; Astruc, D., Atomically precise copper nanoclusters and their applications. *Coord. Chem. Rev.* **2018,** *359*, 112.
(8) Jin, R.; Zeng, C.; Zhou, M.; Chen, Y., Atomically Precise Colloidal Metal Nanoclusters and Nanoparticles: Fundamentals and Opportunities. *Chem. Rev.* **2016,** *116*, 10346.
(9) Parker, J. F.; Weaver, J. E. F.; McCallum, F.; Fields-Zinna, C. A.; Murray, R. W., Synthesis of Monodisperse $[Oct_4N^+][Au_{25}(SR)_{18}^-]$ Nanoparticles, with Some Mechanistic Observations. *Langmuir* **2010,** *26*, 13650.
(10) Zhu, M.; Aikens, C. M.; Hollander, F. J.; Schatz, G. C.; Jin, R., Correlating the Crystal Structure of A Thiol-Protected Au_{25} Cluster and Optical Properties. *J. Am. Chem. Soc.* **2008,** *130*, 5883.
(11) Brennan, J. G.; Siegrist, T.; Kwon, Y. U.; Stuczynski, S. M.; Steigerwald, M. L., Nickel-selenium-triethylphosphine ($Ni_{23}Se_{12}(PEt_3)_{13}$), an intramolecular intergrowth of nickel selenide (NiSe) and nickel. *J. Am. Chem. Soc.* **1992,** *114*, 10334.
(12) Fenske, D.; Krautscheid, H.; Müller, M., New Intermediate Steps in the Synthesis of Larger Nickel Clusters. *Angew. Chem. Int. Ed.* **1992,** *31*, 321.
(13) Wix, P.; Kostakis, G. E.; Blatov, V. A.; Proserpio, D. M.; Perlepes, S. P.; Powell, A. K., A Database of Topological Representations of Polynuclear Nickel Compounds. *Eur. J. Inorg. Chem.* **2013,** *2013*, 520.
(14) Ceriotti, A.; Fait, A.; Longoni, G.; Piro, G.; Demartin, F.; Manassero, M.; Masciocchi, N.; Sansoni, M., Synthesis and x-ray structure of the $[HNi_{38}(CO)_{42}C_6]^{5-}$ cluster: an extended fragment of the $Cr_{23}C_6$ lattice stabilized in a molecular carbonyl nickel cluster. *J. Am. Chem. Soc.* **1986,** *108*, 8091.
(15) Calderoni, F.; Demartin, F.; Iapalucci, M. C.; Longoni, G., Synthesis and Crystal Structure of the $[Ni_{32}C_6(CO)_{36}]^{6-}$ Hexaanion: An Extended Fragment of the $M_{23}C_6$ Lattice Stabilized in a Shell of Edge-Bridging Carbonyl Ligands. *Angew. Chem. Int. Ed.* **1996,** *35*, 2225.
(16) Brennan, J. G.; Siegrist, T.; Stuczynski, S. M.; Steigerwald, M. L., The transition from molecules to solids: molecular syntheses of $Ni_9Te_6(PEt_3)_8$, $Ni_{20}Te_{18}(PEt_3)_{12}$ and NiTe. *J. Am. Chem. Soc.* **1989,** *111*, 9240.
(17) Bencharif, M.; Cador, O.; Cattey, H.; Ebner, A.; Halet, J.-F.; Kahlal, S.; Meier, W.; Mugnier, Y.; Saillard, J.-Y.; Schwarz, P.; Trodi, F. Z.; Wachter, J.; Zabel, M., Electron-Sponge Behavior, Reactivity and Electronic Structures of Cobalt-Centered Cubic $Co_9Te_6(CO)_8$ Clusters. *Eur. J. Inorg. Chem.* **2008,** *2008*, 1959.
(18) Touchton, A. J.; Wu, G.; Hayton, T. W., $[Ni_8(CN^tBu)_{12}][Cl]$: A nickel isocyanide nanocluster with a folded nanosheet structure. *J. Chem. Phys* **2021,** *154*, 211102.
(19) Cook, A. W.; Wu, G.; Hayton, T. W., A Re-examination of the Synthesis of Monolayer-Protected $Co_x(SCH_2CH_2Ph)_m$ Nanoclusters: Unexpected Formation of a Thiolate-Protected Co(II) T3 Supertetrahedron. *Inorg. Chem.* **2018,** *57*, 8189.
(20) Touchton, A. J.; Wu, G.; Hayton, T. W., Generation of a Ni_3 Phosphinidene Cluster from the Ni(0) Synthon, $Ni(\eta^3\text{-}CPh_3)_2$. *Organometallics* **2020,** *39*, 1360.
(21) Touchton, A. J.; Wu, G.; Hayton, T. W., Understanding the Early Stages of Nickel Sulfide Nanocluster Growth: Isolation of Ni_3 , Ni_4 , Ni_5 , and Ni_8 Intermediates. *Small* **2020**, 2003133.
(22) Cook, A. W.; Hayton, T. W., Case Studies in Nanocluster Synthesis and Characterization: Challenges and Opportunities. *Acc. Chem. Res.* **2018,** *51*, 2456.

(23) Narasimhan, L. R.; Palstra, T. T. M.; Tanzler, S. M.; Steigerwald, M. L., Relation between magnetic and structural anisotropy in the $Ni_{23}Se_{12}(PEt_3)_{12}$ cluster compound. *Phys. Rev. B: Condens. Matter Mater. Phys.* **1995,** *51*, 9337.
(24) We believe that the mass spectrometer is the likely source of the Br^- ions observed in the ESI-MS spectrum
(25) Knighton, R. C.; Beer, P. D., Sodium cation-templated synthesis of an ion-pair binding heteroditopic [2]catenane. *Org. Chem. Front.* **2021,** *8*, 2468.
(26) Liu, Y.; Zhao, W.; Chen, C.-H.; Flood, A. H., Chloride capture using a C–H hydrogen-bonding cage. *Science* **2019,** *365*, 159.
(27) Haketa, Y.; Maeda, H., From Helix to Macrocycle: Anion-Driven Conformation Control of π-Conjugated Acyclic Oligopyrroles. *Chem. Eur. J.* **2011,** *17*, 1485.
(28) Hua, Y.; Liu, Y.; Chen, C.-H.; Flood, A. H., Hydrophobic Collapse of Foldamer Capsules Drives Picomolar-Level Chloride Binding in Aqueous Acetonitrile Solutions. *J. Am. Chem. Soc.* **2013,** *135*, 14401.
(29) Lucchese, B.; Humphreys, K. J.; Lee, D.-H.; Incarvito, C. D.; Sommer, R. D.; Rheingold, A. L.; Karlin, K. D., Mono-, Bi-, and Trinuclear Cu^{II}-Cl Containing Products Based on the Tris(2-pyridylmethyl)amine Chelate Derived from Copper(I) Complex Dechlorination Reactions of Chloroform. *Inorg. Chem.* **2004,** *43*, 5987.
(30) Jensen, K. A., Zur Stereochemie des koordinativ vierwertigen Nickels. *Z. Anorg. Allg. Chem.* **1936,** *229*, 265.
(31) Pauling, L., Atomic Radii and Interatomic Distances in Metals. *J. Am. Chem. Soc.* **1947,** *69*, 542.
(32) Fenske, D.; Ohmer, J.; Hachgenei, J., New Co and Ni Clusters with Se and PPh_3 as Ligands: $[Co_4(\mu_3\text{-}Se)_4(PPh_3)_4]$, $[Co_6(\mu_3\text{-}Se)_8(PPh_3)_6]$, $[Co_9(\mu_4\text{-}Se)_3(\mu_3\text{-}Se)_8(PPh_3)_6]$, and $[Ni_{34}(\mu_5\text{-}Se)_2(\mu_4\text{-}Se)_{20}(PPh_3)_{10}]$. *Angew. Chem. Int. Ed.* **1985,** *24*, 993.
(33) Grønvold, F.; Jacobsen, E., X-Ray and Magnetic Study of Nickel Selenides in the l'Range NiSe to $NiSe_2$. *Acta Chem. Scand.* **1956,** *10*, 1440.
(34) Stevels, A. L. N., Phase transitions in nickel and copper selenides and tellurides. *Philips Res. Repts. Suppl.* **1969,** *9*, 1.
(35) Fenske, D.; Hachgenei, J.; Ohmer, J., Novel Cobalt- and Nickel-Clusters with S and PPh_3 as Ligands; Crystal Structures of $[Co_7S_6(PPh_3)_5Cl_2]$, $[Co_6S_8(PPh_3)_6]^+$, $[CoCl_3(THF)]^-$, $[Ni_8S_6Cl_2(PPh_3)_6]$, and $[Ni_8S_5(PPh_3)_7]$. *Angew. Chem. Int. Ed.* **1985,** *24*, 706.
(36) Koenig, S.; Fenske, D., Synthesen und Kristallstrukturen der chalkogenidoverbrückten Nickelclusterverbindungen $[Ni_5Se_4Cl_2(PPhEt_2)_6]$, $[Ni_{12}Se_{12}(P^nPr_3)_6]$ und $[Ni_{18}S_{18}(P^iPr_3)_6]$. *Z. Anorg. Allg. Chem.* **2004,** *630*, 2720.
(37) Schubert, E. M., Utilizing the Evans method with a superconducting NMR spectrometer in the undergraduate laboratory. *J. Chem. Educ.* **1992,** *69*, 62.
(38) Evans, D. F., 400. The determination of the paramagnetic susceptibility of substances in solution by nuclear magnetic resonance. *J. Chem. Soc.* **1959**, 2003.
(39) Evans, C. M.; Evans, M. E.; Krauss, T. D., Mysteries of TOPSe Revealed: Insights into Quantum Dot Nucleation. *J. Am. Chem. Soc.* **2010,** *132*, 10973.
(40) Cecconi, F.; Ghilardi, C. A.; Midollini, S.; Orlandini, A.; Vacca, A.; Ramirez, J. A., Ligand substitution reactions of the nickel–sulphur cluster $[Ni_3S_2(PEt_3)_6]^{2+}$. Phosphorus-31 nuclear magnetic resonance characterization of mono- and di-substituted species and X-ray crystal structure of $[Ni_3(\mu_3\text{-}S)_2(PEt_3)_5Cl]BPh_4$. *J. Chem. Soc., Dalton Trans.* **1990**, 773.

(41) Fenske, D.; Fleischer, H.; Krautscheid, H.; Magull, J., Zur Reaktion von $[MCl_2(PR_3)_2]$ (M = Ni, Pd) mit $E(SiMe_3)_2$ (E = S, Se) Die Kristallstrukturen von $[Ni_3S_2Cl_2(PPh_3)_4]$, $[Pd_3S_2Cl_2(PPh_3)_4]$, $[Ni_3Se_2(SeSiMe_3)_2(P(C_2H_4Ph)_3)_4]$ und $[Pd_3Se_2(SeSiMe_3)_2(PPh_3)_4]$. *Z. Naturforsch., B: J. Chem. Sci.* **1990,** *45*, 127.
(42) Hoveyda, H. R.; Holm, R. H., Characterization of the Self-Condensation Equilibrium of $[Fe_4S_4(SH)_4]^{2-}$: Spectroscopic Identification of a Unique Sulfido-Bridged Acyclic Tricubane Cluster. *Inorg. Chem.* **1997,** *36*, 4571.
(43) Segal, B. M.; Hoveyda, H. R.; Holm, R. H., Terminal Ligand Assignments Based on Trends in Metal−Ligand Bond Lengths of Cubane-Type $[Fe_4S_4]^{2+,+}$ Clusters. *Inorg. Chem.* **1998,** *37*, 3440.

TOC Graphic

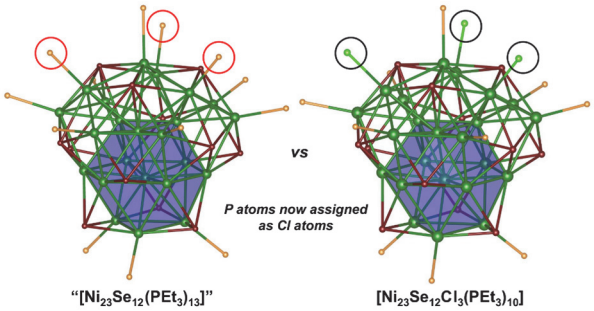

SYNOPSIS. A combined spectroscopic and crystallographic analysis suggests that the previously reported nanocluster $[Ni_{23}Se_{12}(PEt_3)_{13}]$ is better formulated as $[Ni_{23}Se_{12}Cl_3(PEt_3)_{10}]$.